# NKG2D and related immunoreceptors

Roland K. Strong<sup>1\*</sup> and Benjamin J. McFarland<sup>2</sup>

<sup>1</sup>Division of Basic Sciences, Fred Hutchinson Cancer Research Center, 1100 Fairview Ave. North, Seattle, WA 98109

<sup>2</sup>Department of Chemistry and Biochemistry, Seattle Pacific University, 3307 Third Avenue West, Seattle WA 98119

\*email address: RSTRONG@FHCRC.ORG

#### **Abstract**

NK cells are crucial components of the innate immune system, capable of directly eliminating infected or tumorigenic cells and regulating down-stream adaptive immune responses. Unlike T cells, where the key recognition event driving activation is mediated by the unique T cell receptor (TCR) expressed on a given cell, NK cells express multiple activating and inhibitory cell-surface receptors (NKRs), often with overlapping ligand specificities. NKRs display two ectodomain structural homologies, either immunoglobulin- or C-type lectin-like (CTLD). The CTLD immunoreceptor NKG2D is found on NK cells but is also widely expressed on T cells and other immune system cells, providing stimulatory or costimulatory signals. NKG2D drives target cell killing following engagement of diverse, conditionally expressed MHC class I-like protein ligands whose expression can signal cellular distress due to infection or transformation. The symmetric, homodimeric receptor interacts with its asymmetric, monomeric ligands in similar 2:1 complexes, with an equivalent surface on each NKG2D monomer binding extensively and intimately to distinct, structurally divergent surfaces on the ligands. Thus, NKG2D ligand-binding site recognition is highly degenerate, further demonstrated by NKG2D's ability to simultaneously accommodate multiple non-conservative allelic or isoform substitutions in the ligands. In TCRs, 'induced-fit' recognition explains cross-reactivity, but structural, computational, thermodynamic and kinetic analyses of multiple NKG2D-ligand pairs show that rather than classical 'induced-fit' binding, NKG2D degeneracy is achieved using distinct interaction mechanisms at each rigid interface: recognition degeneracy by 'rigid adaptation'. While likely forming similar complexes with their ligand (HLA-E), other NKG2x NKR family members do not require such recognition degeneracy.

#### T cell receptors & MHC class I proteins: paradigms of immunological recognition

Cytotoxic responses by the cellular arm of the adaptive immune system are ultimately mediated by recognition events between αβ T cell receptors (TCRs) on the surfaces of T cells and processed peptide fragments of endogenously expressed proteins, presented to TCRs as complexes on the cell surface with major histocompatibility complex class I proteins (pMHC). Thereby, MHC presentation allows the immune system to monitor the proteome of a given cell for inappropriate protein expression associated with disease (e.g. tumorigenesis or infection). MHC class I proteins are integral-membrane, heterodimeric proteins with ectodomains consisting of a polymorphic heavy chain, comprising three extracellular domains ( $\alpha 1$ ,  $\alpha 2$  and  $\alpha 3$ ), associated with a non-polymorphic light chain,  $\beta_2$ -microglobulin  $(\beta_2 m)^2$ . Association with both peptide and  $\beta_2 m$  is required for normal folding and cell-surface expression. The α1 and α2 domains together comprise the peptide- and TCR-binding 'platform' domain; the α3 and β<sub>2</sub>m domains display C-type immunoglobulin folds. The canonical MHC class I platform fold comprises two long, roughly parallel,  $\alpha$ -helices, interrupted by bends, arranged on an eight-stranded, anti-parallel  $\beta$ -sheet. These  $\alpha$ -helices define the 'walls' of the peptide binding groove. Crystal structures of TCR-pMHC complexes show that the TCR variable domains generally sit diagonally on the platform domain, making contacts to the peptide and the  $\alpha 1$  and  $\alpha 2$  domains (Fig. 14.1; see also Chapter 19 in this volume).3 T cell activation requires an interaction between TCRs and appropriate target pMHC complexes in the context of appropriate co-receptor interactions (e. g. CD4 or CD8) and co-stimulatory signals from, for example, engagement of the CD28 receptor on T cells with CD80 or CD86 ligands on target cells,<sup>4</sup> all stabilized and organized by cell-cell adhesion interactions.<sup>5</sup> Diverse cell-surface molecules that modulate T cell activation also include receptors first identified on natural killer (NK) cells that have since been found expressed on a range of cell types, including T cells (such as NKG2D, see below). The experimentally-observed cross-reactivity of TCR-pMHC interactions is best explained by conformational plasticity, or 'induced-fit' recognition, where a flexible binding site can be molded to accommodate structural diversity across multiple ligands, typified by many antibody-antigen interactions.<sup>7,89</sup>

# NK cells & receptors

NK cells constitute an important component of the innate immune system, providing surveillance against cells undergoing tumorigenesis or infection (by viruses or internal pathogens), without requiring prior host sensitization. NK cells act to regulate innate and acquired immune responses through the release of various immune modulators, such as interferon-γ (IFN-γ), or by direct elimination of compromised cells.<sup>10, 11</sup> NK effector functions are regulated through a diverse array of cell-surface inhibitory and activating receptors (Table 14.1).<sup>11-13</sup> Different NKRs, with different MHC class I specificities, are expressed on overlapping, but distinct, subsets of NK cells. Many NK cell surface receptors (NKRs) are specific for classical (HLA-A, -B and -C) and non-classical (HLA-E) MHC class I proteins and occur in paired activating and inhibitory isoforms.<sup>14</sup> Thus, NK cell effector functions are regulated by integrating signals across the array of activating and inhibitory NKRs engaged upon interaction with target cell-surface NKR ligands,<sup>12, 15, 16</sup> resulting in the elimination of cells with reduced MHC class I expression, a common consequence of infection or transformation.<sup>17</sup>

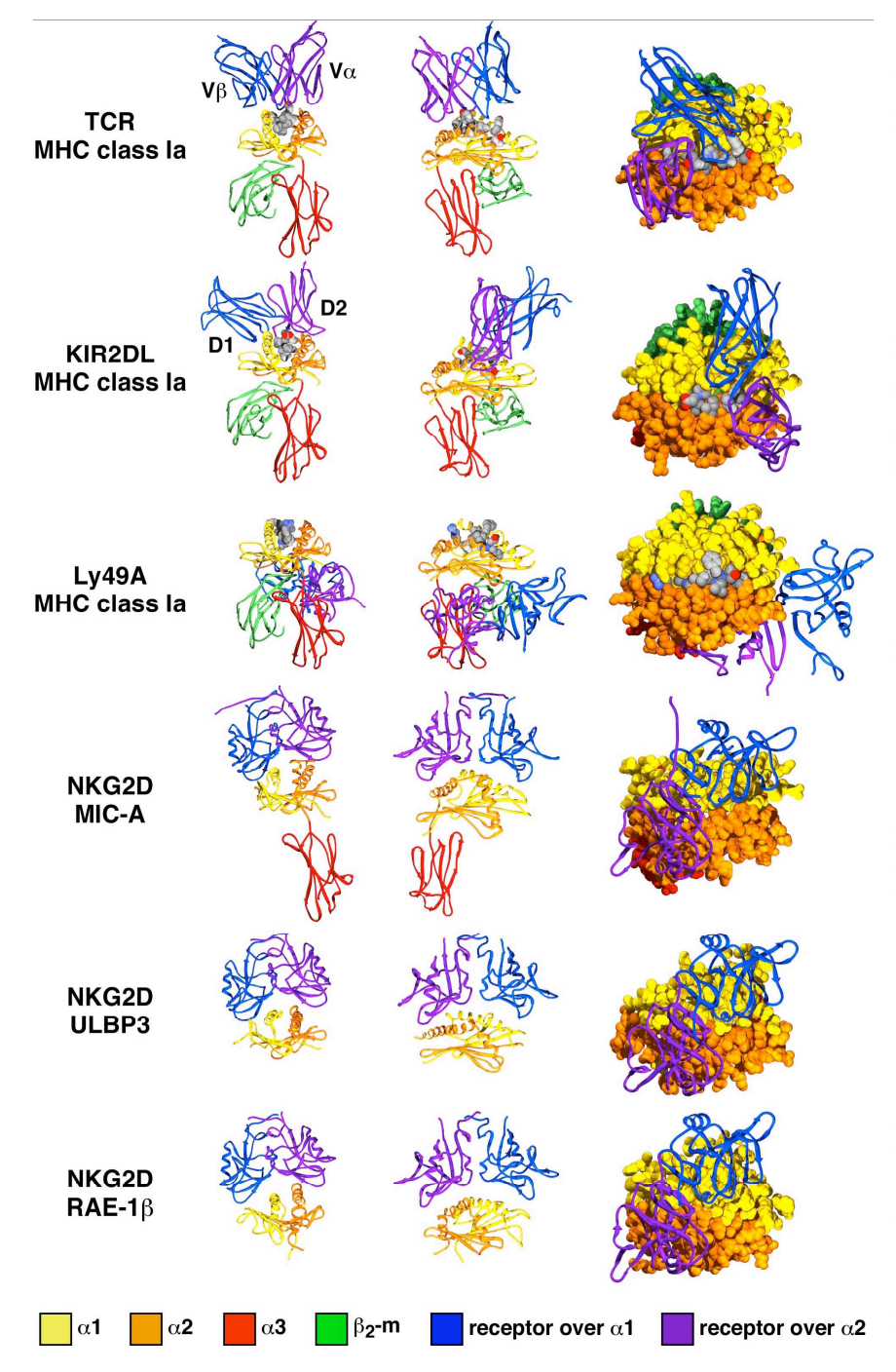


Figure 14.1

Representative immunoreceptorligand complex structures. Views of a series of immunoreceptorligand complexes are shown, in a mix of ribbon and space-filling representations, highlighting the range of variation in these recognition events: α β TCR-classical pMHC class I;<sup>18</sup> KIR2DL-classical pMHC class I;<sup>19</sup> Ly49A–classical pMHC class huNKG2D-MIC-A;<sup>21</sup>  $I^{20}$ huNKG2D-ULBP3;22 a n d muNKG2D-RAE-β.<sup>23</sup> The views in the left-hand column are aligned looking down along the peptide-binding groove (when present). The views in the middle column are perpendicular to the dyad axis of the NKG2D receptor (a rotation of approximately 50° from the view in the left-hand column). The views in the righthand column are oriented looking down onto the top (peptidebinding) surface of the platform domains of the MHC class I protein or homolog (a rotation of 90° from the view in the middle

column). All the molecules in a column are aligned on the platform domain of the MHC class I protein or homolog. Domains are colored as indicated, with the receptors colored in blue and purple and the ligand proteins colored in yellow, orange, red and green; peptides, when present, are colored by atomtype (carbon: gray; oxygen: red; nitrogen: blue; and sulfur: yellow).

**Table 14.1** Properties of immunoreceptors.

Receptor	Structure	Ligand	$K_{D}(\mu M)$	Signal	
Human					
αβ TCRs	IgSF	pMHC class Ia	1 - 90	activation	
CD8	IgSF	pMHC class Ia	65 - 200	(activation)	
γδ TCRs	IgSF	prenyl pyrophosphates;	~0.001 - 103	activation	
		alkamines			
KIRs	IgSF	pMHC class Ia	~10	activation or inhibition	
LIR-1/ILT-2	IgSF	pMHC class Ia	15 - 100	inhibition	
Nkp30, 44 & 46	IgSF	tumor antigens?;	?	activation	
		viral proteins?			
NKG2A-CD94	CTLD	HLA-E	0.36 - ≥34	inhibition	
NKG2C-CD94	CTLD	HLA-E	2.3 - ≥56	activation	
NKG2D	CTLD	(Table 14.2)	(Table 14.2)	activation	
NKG2E-CD94	CTLD	HLA-E ?		activation	
Mouse					
Ly49s	CTLD	pMHC class Ia;	~10	activation or inhibition	
		viral proteins			
NKG2A-CD94	CTLD	Qa-1	?	inhibition	
NKG2C-CD94	CTLD	Qa-1	?	activation	
NKG2D	CTLD	(Table 14.2)	( <i>Table 14.2</i> )	activation	
NKG2E-CD94	CTLD	Qa-1	?	activation	

NKRs can be divided into two families based on structural homologies (Table 14.1). The first family, including the human 'killer cell immunoglobulin' receptors (KIRs)<sup>24</sup> and consists of type I transmembrane glycoproteins containing one to three tandem immunoglobulin-like domains in the ectodomain. The second NKR family comprises homo- and heterodimeric type II transmembrane glycoproteins containing C-type lectin-*like* domains (CTLDs) in their ectodomains and includes the murine Ly49 family<sup>25</sup> and the human and murine-expressed NKG2x NKRs (x = A, B, C, D, E, F & H).<sup>26</sup>, C-type lectin-like receptors are structurally distinct from true, carbohydrate-binding C-type lectins and lack elements associated with specific carbohydrate recognition (Fig. 14.2).<sup>26</sup>, The canonical C-type lectin fold comprises two  $\alpha$ -helices packed against two  $\beta$ -sheets, linked through two invariant disulfide

bonds. A third conserved disulfide bond is found in an N-terminal extension defining the long-form animal C-type lectins; multiple disulfide bonds are found in the analogous extension common to CTLD NKRs (Fig. 14.2).

The number of KIR or Ly49 genes in a particular person or mouse strain varies widely, with around ten expressed in any given individual.<sup>29, 30</sup> Single NK cells within a particular individual typically express from one to five different NKRs,<sup>31, 32</sup> yielding distinct KIR/Ly49-NKG2x combinations.<sup>16</sup> How the particular repertoire of NKRs expressed on a particular NK cell is acquired is still unclear,<sup>12</sup> though it has been demonstrated that NK cells do functionally adapt to the MHC class I environment of the host.<sup>33</sup>

Inhibitory NKRs contain 'immunoreceptor tyrosine-based inhibition motifs' (ITIMs, typically V/IxYxxL sequences) in their endodomains; activating receptors associate with adaptor proteins (typically through complementary charge—charge interactions within transmembrane-spanning domains) containing 'immunoreceptor tyrosine-based activation motifs' (ITAMs, typically YxxL/Ix6-8YxxL/I) or related sequence motifs (YxxM in DAP10, for instance). <sup>12, 13</sup> ITIMs with phosphorylated tyrosines signal inhibition through the recruitment and activation of the SHP-1 phosphatase; ITAMs with phosphorylated tyrosines signal activation through the recruitment of Syk or ZAP70 tyrosine kinases.

# NKG2x NK cell receptors

The NKG2x NKR family can be further subdivided, structurally, functionally and by sequence relationship (Figs. 14.3 and 14.4), into two arms: the closely-related receptors NKG2A, B, C, E, F and H, and the more distantly-related receptor NKG2D. NKG2D is a homodimeric, activating, CTLD-type immunoreceptor whose expression was first recognized on NK cells but was subsequently found on CD8-positive αβ T cells, γδ T cells and macrophages, making it one of the most widely distributed NKRs currently described.<sup>34,35</sup> The other members of the NKG2x family (A, B, C, E & H) form obligate heterodimers with CD94, are highly homologous to each other (Figs. 14.3 and 14.4), are limited in expression to NK cells and are specific for the non-classical MHC class I protein HLA-E in humans or Qa-1 in mice (Table 14.1). 16, 36 The exception to this generalization may be NKG2F, which has not been demonstrated to be expressed on cell surfaces and is missing large, otherwise-conserved sections of the CTLD, but which does contain a cytoplasmic ITIM-like sequence.<sup>37</sup> HLA-E binds peptides, like the classical MHC class I (or class Ia) proteins, though with a much more restricted specificity, 38, 39 limited essentially to fragments of the leader sequences of MHC class I proteins. 40 Therefore, normal HLA-E cell-surface expression is an indirect check for the normal expression of MHC class I proteins. NKG2A/B and NKG2E/H are splice variants, 41, 42 where the only resultant differences are that NKG2H has a longer (+16 residues), and different, C-terminal extension than NKG2E compared to the rest of the family; and that NKG2B has a truncated extracellular, N-terminal 'arm' relative to NKG2A (which is also shorter than in any other family member). This arm spans the distance between CTLD and the transmembrane domain in NKG2x NKRs. The inhibitory NKG2x NKRs (A/B) have two ITIMs in their endodomains; the activating NKG2x NKRs (C & E/H, but not D), as well as many of the activating immunoglobulin-type NKRs, interact with the DAP12 adaptor (also known as KARAP). 43,44

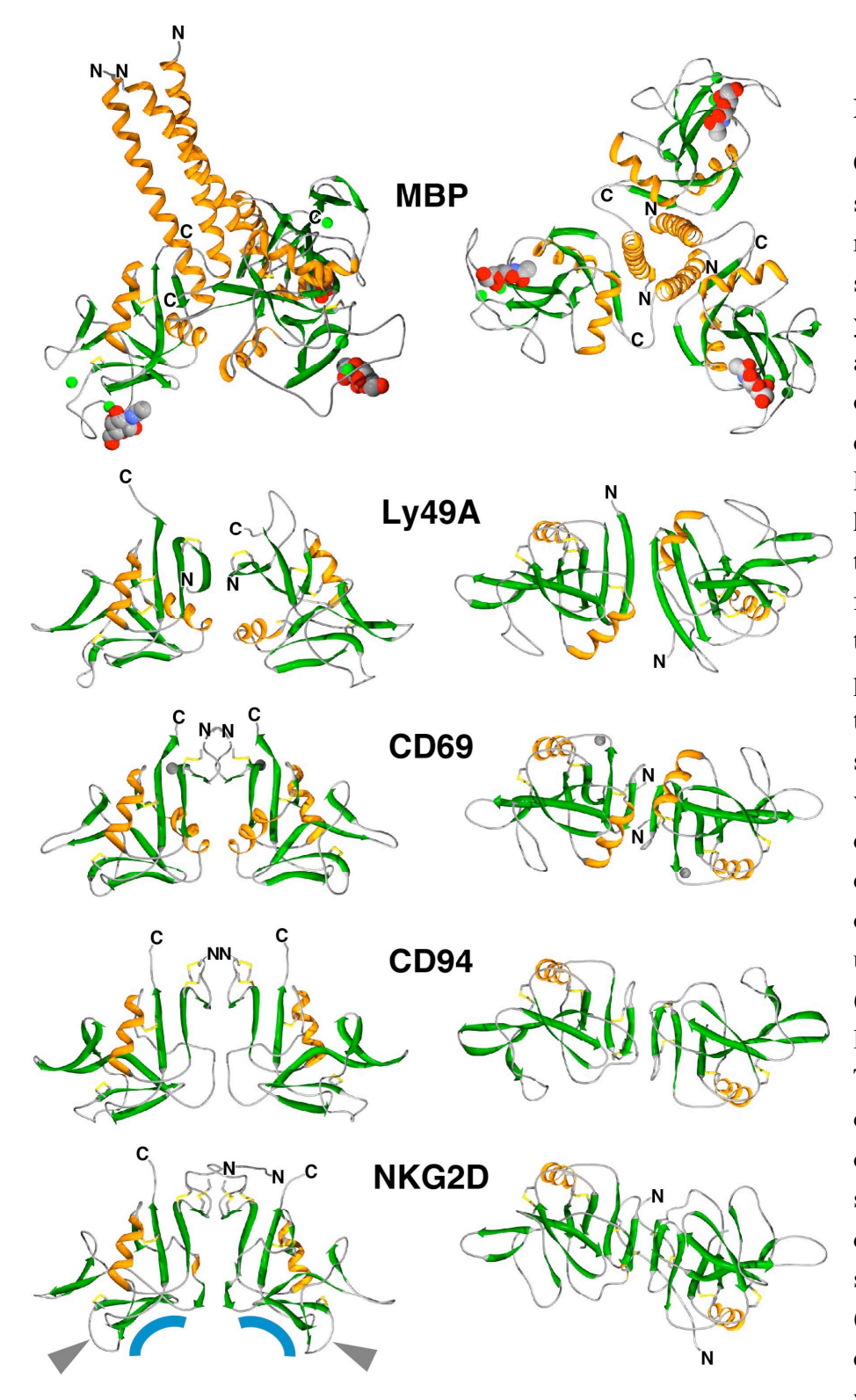
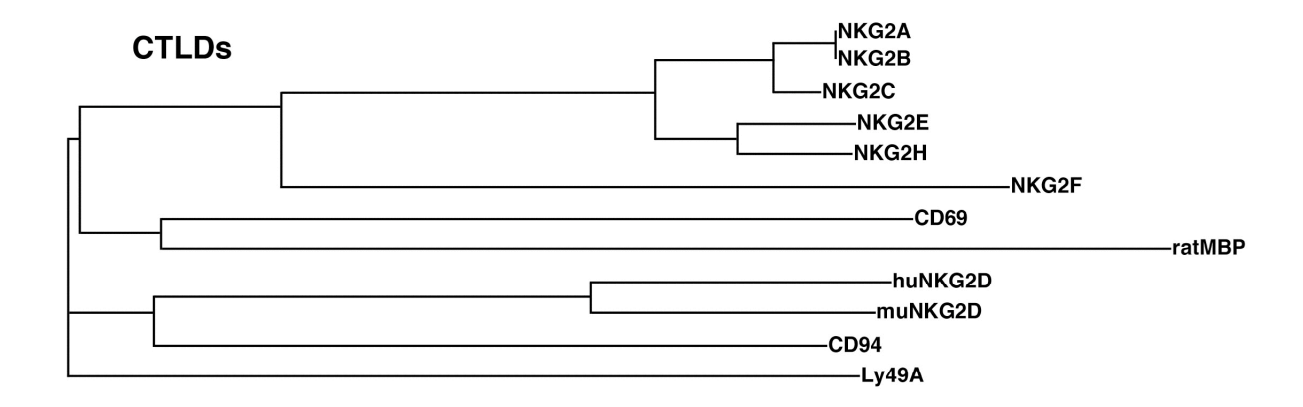


Figure 14.2

Comparison of **CTLD** structures. Ribbon representations, colored secondary structure (α-helices: yellow coils; β-strands: green arrows), are shown for a series ofillustrative CTLDcontaining immunoreceptors: Ly49A,20 CD69,45 CD946 and huNKG2D.47 The structure of the archetype C-type lectin fold-containing protein, trimeric rat mannose binding protein (MBP), is shown at the top for comparison.48 The structures are shown in two views, one perpendicular to the dyad axis of symmetry in the dimeric molecules (left) and one view from below, looking up onto the ligand binding sites (right; 90° from the view on the left for the dimeric molecules). The left-hand views are oriented so that the left CTLD or C-type lectin domains are superimposed, highlighting the differences in the fold of the short-form C-type lectins (MBP) and the CTLDcontaining immunoreceptors, which are more homologous to

long-form C-type lectins. N- and C-termini are labeled. A disaccharide ligand is shown (in a space-filling representation, colored by atom-type as in Fig. 14.1) for MBP; the NKG2D ligand-binding site is indicated with blue arcs. Bound ions are shown as spheres: calcium atoms (green) in the MBP structure; zinc atoms (gray) in CD69. The gray pointers mark the NKG2D stirrup loops, a structurally divergent feature of NKG2D that results in the distinctly saddle-shaped ligand-binding surface of this NKR.



NIZCOD

NIZCOD

	NKG2A	NKG2B	NKG2C	(human)	(murine)	NKG2E	NKG2F	NKG2H	CD94	CD69	Ly49A	MBP
NKG2A	100	100	94	25	23	81	39	81	25	26	29	13
NKG2B	100*	100										
NKG2C	68	66	100	25	23	83	39	83	25	26	30	12
NKG2D (human)	8	33	18	100	72	20	17	20	32	21	25	7
NKG2D (murine)	8	33	9	42	100	22	15	27	35	21	27	7
NKG2E	73	50	94	10	10	100	39	88	24	24	28	11
NKG2F	54	66	68	8	8	68	100	39	23	17	15	3
NKG2H	73	50	94	10	10	100*	68	100	28	22	26	11
CD94	16	16	22	11	11	26	16	26	100	22	24	15
CDEO	1	16	1	1	0	Ę.	n	F	n	100	က	16

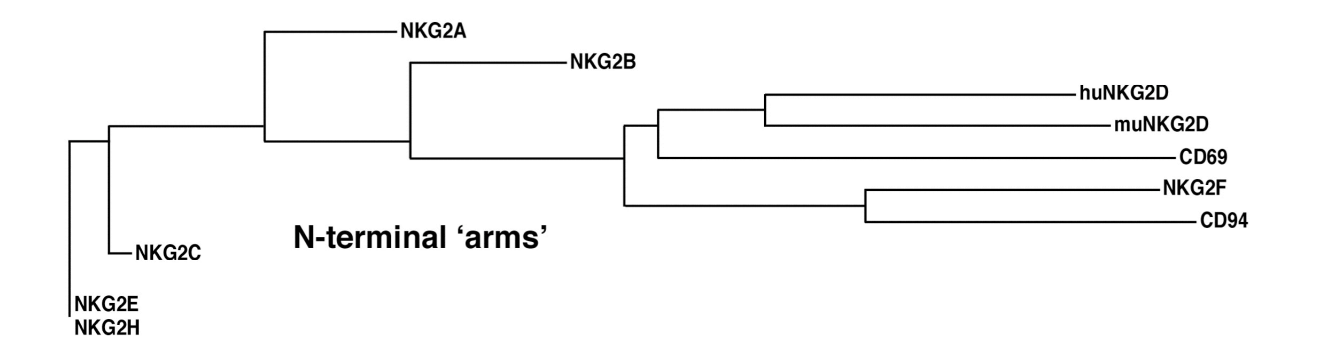


Figure 14.3

CTLD/N-terminal arm sequence identities & phylogenies. Sequence phylogenies (top and bottom) and identities (middle) between the CTLDs (top and top-right half of middle panel) or the N-terminal arms (bottom and bottom-left half of middle panel) of the NKG2x NKRs, CD69, CD94 and Ly49A. In the middle panel, fewer values are shown for the CTLD of NKG2B, as this splice variant is identical to NKG2A in the CTLD, or for the N-terminal arm of Ly49A, which shows no meaningful similarity to the arms of the other receptors. Identities and phylogenies were calculated with CLUSTALW.<sup>49</sup>

NKG2D displays only limited sequence similarity to other NKG2x family members and CD94 (Figs. 14.3 and 14.4), has not been demonstrated to directly interact with MHC class I proteins and only forms obligate homodimers.<sup>21, 50</sup> Human NKG2D (huNKG2D) engagement is signaled by recruitment of phosphatidylinositol 3-kinase and Grb2 through the adapter molecule DAP10,<sup>35, 51</sup> whereas different splice variants of murine NKG2D (muNKG2D) have been reported to utilize both DAP10 and DAP12, perhaps in functionally-distinct contexts.<sup>52, 53</sup>

### HuNKG2D ligands: MIC-A/B

HuNKG2D ligands (Table 14.2) include the closely related proteins MIC-A and MIC-B (MHC class I chain-related)<sup>54-56</sup> and the ULBPs (human cytomegalovirus (CMV) <u>UL</u>16-binding proteins).<sup>57</sup> All are distant MHC class I homologs that do not function in conventional peptide antigen presentation. HuNKG2D–MIC recognition events stimulate effector responses from NK cells (calcium fluxing, production of IFN-γ, GM-CSF, TNF-α and -β, and MIP-1β) as well as γδ T cells and may positively modulate CD8-positive αβ T cell responses, thus serving a co-stimulatory function.<sup>34, 58</sup> On macrophages, stimulation through huNKG2D triggers TNF-α production and release of nitric oxide.<sup>59</sup> On NK cells, stimulation through NKG2D alone is sufficient to trigger effector functions.<sup>60</sup> The NKG2D activation signal can override inhibitory signals that would otherwise prevent activation<sup>34, 59, 61, 62</sup> but apparently not in all contexts.<sup>63</sup>

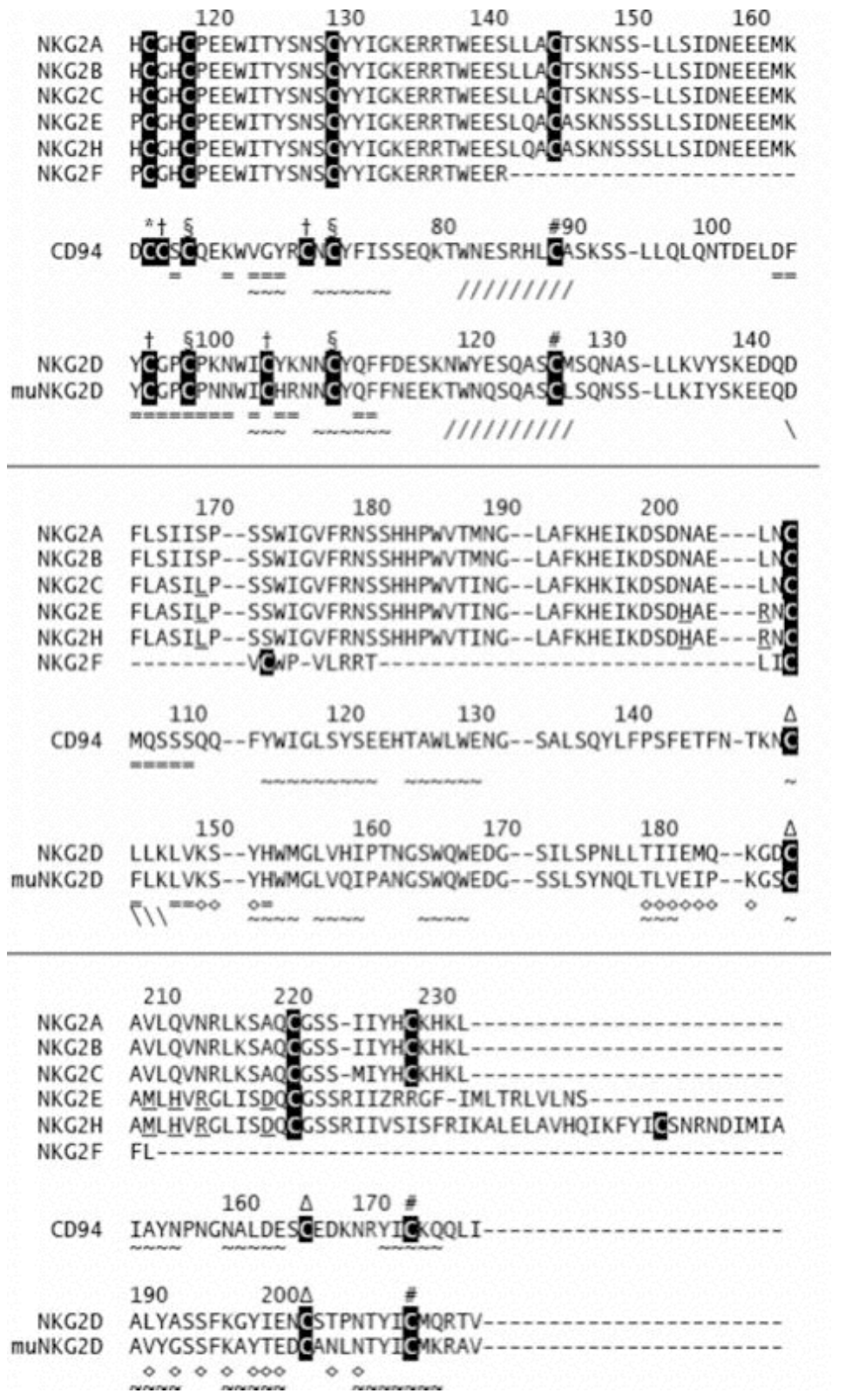
Unlike the widely- and constitutively-expressed classical and non-classical MHC class I proteins, MIC-A and MIC-B are induced only in response to cellular stress on intestinal epithelium, epitheliallyderived tumors and vascular endothelium.<sup>56, 64</sup> While MIC-A and MIC-B are quite similar to each other (~84% identical; Fig. 14.5),<sup>55, 65</sup> they have diverged significantly from the MHC class I family as a whole, with identities of approximately 28% to 35% domain-by-domain when aligned with the human MHC class I proteins. MIC-A and -B are highly polymorphic, with over fifty MIC-A and thirteen MIC-B alleles recognized, numbers that continue to increase. 66 The polymorphisms are spread over the extracellular domains of the proteins, and are predominantly the result of single amino acid substitutions that generate dimorphic positions (Fig. 14.5). Many of these changes are non-conservative and the pattern of sequence variation is wholly distinct from that for the classical MHC class I proteins - a pattern not readily rationalizable in terms of known interactions with any of its receptors. 67 MIC-A/B proteins are conserved in most mammals except rodents. MIC proteins do not require either peptide or β<sub>2</sub>m for stability or cell-surface expression and apparently do not bind any other ligand in the shallow pocket that represents the only remnant of the peptide-binding groove of true MHC class I proteins.<sup>56, 67</sup> Human tumors are capable of evading NKG2D-mediated immunosurveillance by shedding soluble forms of MIC proteins that down-regulate of NKG2D on effector cells. 68,69

Table 14.2 NKG2D ligansds & affinities

Ligand	Domain Structure	e K <sub>D</sub> (μM)	Expression	Inducers
Human				
MIC-A	$(\alpha 1\alpha 2)\alpha 3$ -TM	0.3 - 0.94	intestinal epithelium;	cellular stress;
			tumors	tumorigenesis; infection
MIC-B	$(\alpha 1\alpha 2)\alpha 3$ -TM	0.79	intestinal epithelium;	cellular stress;
			tumors	tumorigenesis; infection
ULBP1	(α1α2)-GPI	1.1	kidney? thyroid?	?
ULBP2	(α1α2)-GPI	?	?	?
ULBP3	(α1α2)-GPI	4.0	kidney?	?
ULBP4	(α1α2)-GPI	?	?	?
Mouse				
RAE-1α	(α1α2)-GPI	0.42 - 0.59	onco-fetal	retinoic acid; carcinogens
RAE-1β	(α1α2)-GPI	0.57 - 1.9	onco-fetal	retinoic acid; carcinogens
RAE-1γ	(α1α2)-GPI	0.35 - 0.38	onco-fetal	retinoic acid; carcinogens
RAE-1δ	(α1α2)-GPI	0.73 - 1.0	onco-fetal	retinoic acid; carcinogens
RAE-1ε	(α1α2)-GPI	?	?	retinoic acid?
RAE-1B	6 (α1α2)-GPI	0.028 - 0.034	?	retinoic acid?
H60	$(\alpha 1\alpha 2)$ -TM	0.014 - 0.027	?	carcinogens
MULT1	$(\alpha 1\alpha 2)$ -TM	0.0015 - 0.0056	?	?

#### **HuNKG2D ligands: ULBPs**

ULBPs are homologous to the α1α2 peptide-binding platform domains of MHC class I proteins, but lack α3 domains, and are anchored in the membrane by GPI-linkages. ULBP1, 2, 3 and 4 (Table 14.2, Fig. 14.6) are 20 to 27% identical in sequence to MIC-A, MIC-B or classical MHC class I proteins.<sup>57</sup> The functional significance of the huNKG2D–ULBP interaction remains to be determined, though human CMV UL16–ULBP and UL16–MIC binding may block huNKG2D–ULBP and huNKG2D–MIC interactions, thus potentially representing a viral strategy to mask these antigens, preventing activation through NKG2D and limiting anti-viral innate immune responses.<sup>57</sup> Alternately, UL16 binding may act by retaining NKG2D, MIC-B, and ULBP 1 and 2 (but apparently not other NKG2D ligands) in the endoplasmic reticulum, preventing their cell-surface expression and function.<sup>70</sup>



### Figure 14.4

NKG2x NKR sequence alignments. Sequences of the NKG2x NKRs and CD94 have been aligned using CLUSTALW.49 Sequences have been numbered from the initiator methionine in the leader peptide, but only the residues in the mature ectodomain CTLDs are shown. Cysteines have been highlighted and disulfide bond partners have been indicated with matching symbols (\*,  $\dagger$ ,  $\S$ , #,  $\Delta$ ), but only when based on crystallographic data. Below each sequence, receptor dimer contacts (=), ligand contacts (\$\daggerightarrow\$) and secondary structure element (α-helix: /; β-strand:  $\sim$ ;  $3_{10}$ -helix:  $\rangle$ ) are indicated with symbols.

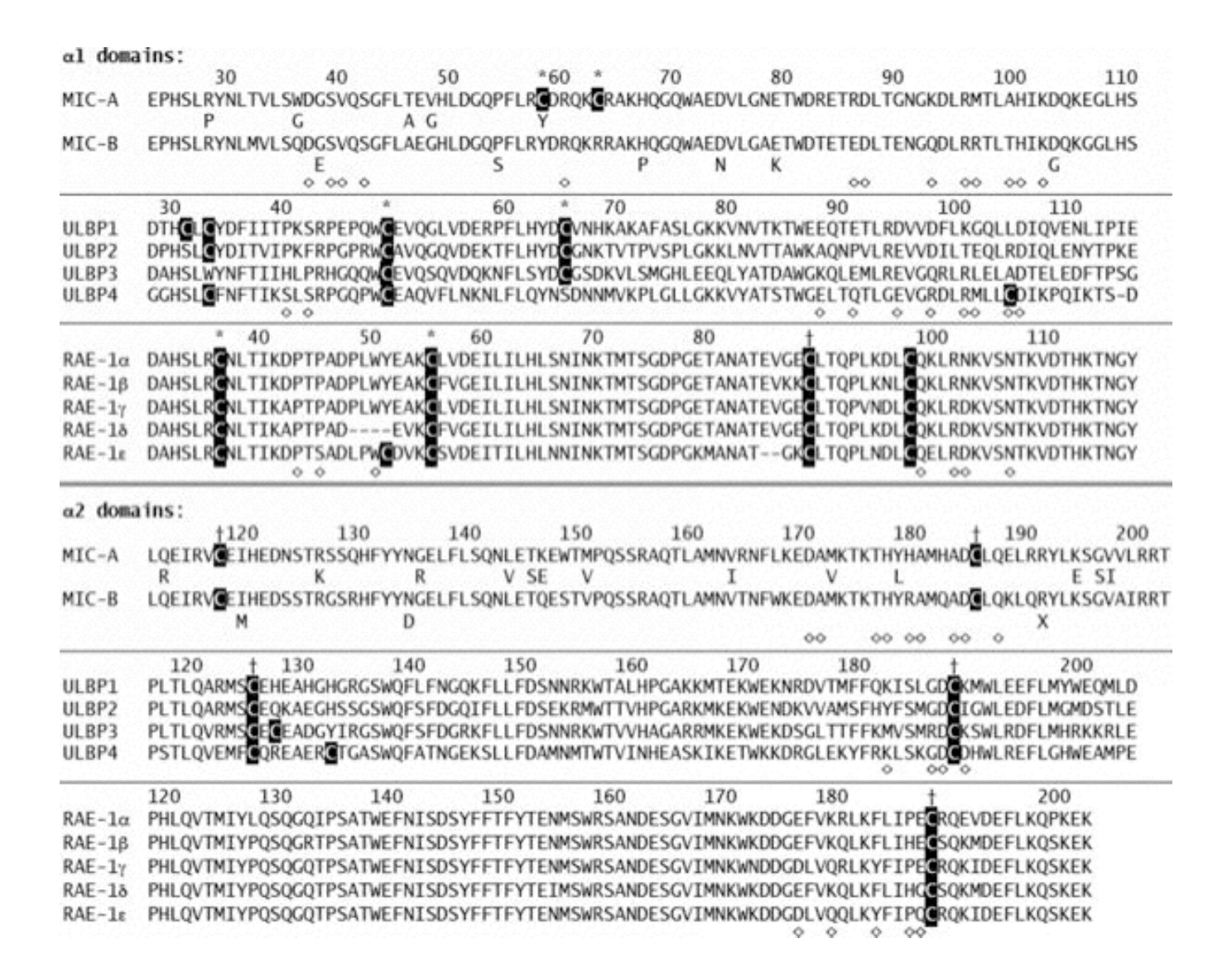


**Figure 14.5** 

Platform sequence alignments of the MHC class I-like ligands of NKG2D. Sequences of MIC-A and -B, the ULBPs and the RAE-1s have been aligned, divided by family and domain, using CLUSTALW. Note that the alignments across families are only very approximate at these levels of sequence identity. Sequences have been numbered from the initiator methionine in the leader peptide, but only the residues in the mature proteins have been shown. Cysteines have been highlighted, and disulfide bond partners have been indicated with matching symbols (\*, †). For the MIC sequences, allelic substitutions have been indicated by the additional residues shown below the sequences (deletions are indicated with an 'X'). Diamonds below the sequences indicate NKG2D contact positions, based on the known complex structures (MIC-A\*001, ULBP3 and RAE-1β).

#### MuNKG2D ligands: RAE-1s, H60 & MULT1

Rodents lack any recognizable homologs of MIC-A/B, but muNKG2D ligands do include the RAE-1 (retinoic acid early inducible) family of proteins, H60 and the recently described MULT1 (Table 14.2).<sup>59</sup>, <sup>61, 71, 72</sup> Like the ULBPs, RAE-1 and H60 are homologous to the platform domains of MHC class I proteins (RAE-1 is 19 to 20% identical to a bovine MHC class I protein), <sup>71</sup> lack α3 domains, and are also anchored in the membrane by GPI-linkages. RAE-1 and H60 show only weak homology to each other (approximately 24%) or to MIC-A and MIC-B (approximately 20%).<sup>61</sup> The RAE-1 family comprises five highly-homologous isoforms ( $\geq$ 89% identical; Fig. 14.6), RAE-1 $\alpha$ ,  $\beta$ ,  $\gamma$ ,  $\delta$  and  $\epsilon$ , which are highly expressed during embryonic development and upregulated on multiple tumor types, but are rare in normal adult tissues. 59, 62, 71, 73-75 It has been shown that tumors expressing RAE-1 molecules can be recognized by NK cells and rejected.<sup>62</sup> Like huNKG2D-MIC stimulation of NK cells, RAE-1 mediated rejection can override inhibitory signals from the expression of self MHC class I proteins on tumor cells. H60 was originally identified as an immunodominant minor histocompatibility antigen. 76, 77 Though differentially expressed in inbred mouse strains, H60 transcripts were found present at low levels in embryonic tissue and on activated thymoblasts, but at higher levels on macrophages and dendritic cells in the spleen and some tumor cells.<sup>15, 59, 76, 77</sup> Little is known about the function of MULT1, but it is apparently widely and constitutively transcribed.<sup>72</sup>

Therefore, NK cells mediate potent anti-tumor and anti-viral responses, either through *i*) recognition of the loss of expression of the normal complement of classical and non-classical MHC class I proteins on cell surfaces or by *ii*) recognition of the induced expression of cell-surface markers of cellular 'distress' (responses to tumorigenesis or infection). These mechanisms can also contribute to significant NK-mediated graft-versus-leukemia responses during non-myeloablative allogeneic stem cell transplantation.<sup>78</sup>

#### **NKG2D-ligand complexation**

The symmetric NKG2D homodimers bind their asymmetric, monomeric ligands (MIC-A, ULBP3 and RAE-1 $\beta$ ) in a 2:1 molar stoichiometry (Fig. 14.1). Equivalent binding sites on each NKG2D monomer contribute nearly equally to an extensive interface (buried solvent accessible surface areas from 1,681 to 2,282Ų) where each receptor monomer binds a distinct ligand surface (Fig. 14.1). The interfaces encompass a mix of bonding interactions (Figs. 14.7 and 14.8) where neither electrostatic nor hydrophobic terms dominate. All three NKG2D complexes are quite similar overall, despite the dissimilarity in detail between the structures of the ligand proteins (ligand structural differences are large enough to almost preclude meaningful rmsd calculations²³). The saddle-shaped NKG2D homodimer sits astride the platform domain of the MHC class I-like ligands, with each NKG2D monomer primarily contacting either the  $\alpha$ 1 or  $\alpha$ 2 sub-domain of each ligand. Shape complementarities²9 are quite high (0.63 to 0.72) and sufficient to exclude water molecules from the interfaces. The NKG2D footprint on its MHC class I-like ligands (Fig. 14.1) overlaps the footprints of  $\alpha$ 8 TCRs and KIR NKRs on MHC

	ULBP1	ULBP2	ULBP3	ULBP4
ULBP1	100	59	54	35
ULBP2		100	54	30
ULBP3			100	33
ULBP4				100

	RAE-1α	RAE-1β	RAE-1γ	RAE-1δ	RAE-1ε
RAE-1α	100	94	94	93	89
RAE-1β		100	92	95	89
RAE-1γ			100	92	92
RAE-1δ				100	89
RAE-1ε					100

Figure 14.6

ULBP and RAE-1 sequence relationships. Sequence identities between members of the ULBP (left) or RAE-1 (right) families are tabulated. Identities were calculated with CLUSTALW.<sup>49</sup>

class Ia proteins, but is distinct from that of murine Ly49 NKRs or LIR- $1^{80}$  on their MHC class Ia ligands.

In these complexes, each NKG2D monomer–ligand subdomain ( $\alpha 1$  or  $\alpha 2$ ) pair is referred to as a 'half-site'. The footprints of the ligands on each of the six NKG2D half-sites essentially overlap, showing that NKG2D truly utilizes a single binding site consisting of residues from the body of the NKG2D CTLD and one loop (Fig. 14.7). This loop, referred to as the 'stirrup' loop<sup>21</sup> (Fig. 14.1), is the most extended element of NKG2D that contacts ligand. The conformation of this loop, distinct from other CTLD structures (Fig. 14.2), gives the ligand-binding surface on NKG2D its distinctive concave curvature. Stirrup loop sequence differences between muNKG2D and huNKG2D result in different overall curvatures, contributing to altered ligand preferences between these two orthologs at a very coarse structural level: huNKG2D will bind the narrow platforms of MIC and ULBP proteins, but not the broader RAE-1s (Fig. 14.7); the more splayed muNKG2D homodimer will bind human ligands as well, consistent with the conservation of the key ligand-binding residues between the human and murine receptors.<sup>47</sup>

The single NKG2D binding site has therefore evolved to recognize at least six different surfaces, predominantly on the α1 or α2 domains of MIC-A, ULBP3 and RAE-1β, with dramatically different shapes. The degree of this extreme recognition degeneracy is further magnified as many of the very nonconservative sequence differences and deletions between MIC-A and -B alleles, and ULBP and RAE-1 isoforms, map to NKG2D-contacting residues on the ligand proteins (Fig. 14.7).<sup>22, 23, 67</sup> NKG2D's interaction with the highly-divergent, and, therefore, likely structurally-distinct, ligand H60 is also yet to be characterized, but would be predicted to display yet additional examples of NKG2D recognition degeneracy. The diversity of interfacial contacts ensures that NKG2D recognition degeneracy is not the product of a dominantly hydrophobic or electrostatic binding site, relatively geometry-insensitive bonds that otherwise enable degenerate recognition in other systems.

## NKG2D-ligand recognition degeneracy: 'rigid adaptation' rather than 'induced-fit'

In contrast to TCR-pMHC and other NK receptor-ligand interactions, and consistent with comparisons of bound and unbound NKG2D structures, 47 thermodynamic and kinetic analyses of four NKG2D-ligand pairs (MIC-A\*001, MIC-B\*005, ULBP1 and RAE-1β) also show that the enthalpic and entropic terms of binding, heat capacities, association rates and activation energy barriers are comparable to typical, rigid protein-protein interactions and distinct from the values associated with classical definitions of induced-fit binding (Figs. 14.9 and 14.10). 81 NKG2D degeneracy is alternatively achieved by employing distinct interaction mechanisms at each rigid interface. At the center of the NKG2D binding site lie two conserved tyrosine residues (152 and 199 in huNKG2D and 168 and 215 in muNKG2D) that constitute the dominant binding-energy 'hotspots'82 in each complex half-site (Fig. 14.7).<sup>47</sup> These two tyrosines are held fairly rigidly in the NKG2D structure, where the only significant conformational change observed is utilization of a single alternate rotamer by Tyr152 in two of the total of eight independent crystallographic views of the NKG2D monomer (two NKG2D monomers in each complex structure plus one monomer each in the free muNKG2D and huNKG2D structures).<sup>47</sup> The conformational plasticity associated with induced-fit binding often encompasses backbone movements of six ångstroms or more, well beyond the scale of the side-chain 'wiggle' observed among NKG2D structures. As has been seen in many antibody combining sites, 83, 84 these tyrosines make multifarious interactions among the distinct ligand surfaces: conserved and non-conserved hydrogen bonds, differential hydrophobic interactions with a range of residues, ring/ring-stacking interactions and even cation- $\pi$  bonds.

NKG2D's extreme recognition degeneracy is therefore achieved by investing a significant proportion of the binding energy in core residues that, while rigidly constrained, are capable of making specific, yet disparate, interactions with the divergent ligand binding surfaces. These core interactions are placed within the context of extensive, water-excluding, highly shape-complementary interfaces, where additional electrostatic, hydrogen and van der Waals bonds contribute to the overall affinity while minimizing the dominance of any single peripheral contact (Figs. 14.8 and 14.11). The extent of the interfaces contributes to affinity and specificity by enabling multiple peripheral bonds to add to affinity, but also by requiring that potential target ligands stringently exclude deleterious steric clashes, both on the scale of individual side-chains and in the overall shape of the NKG2D binding saddle.<sup>47</sup>

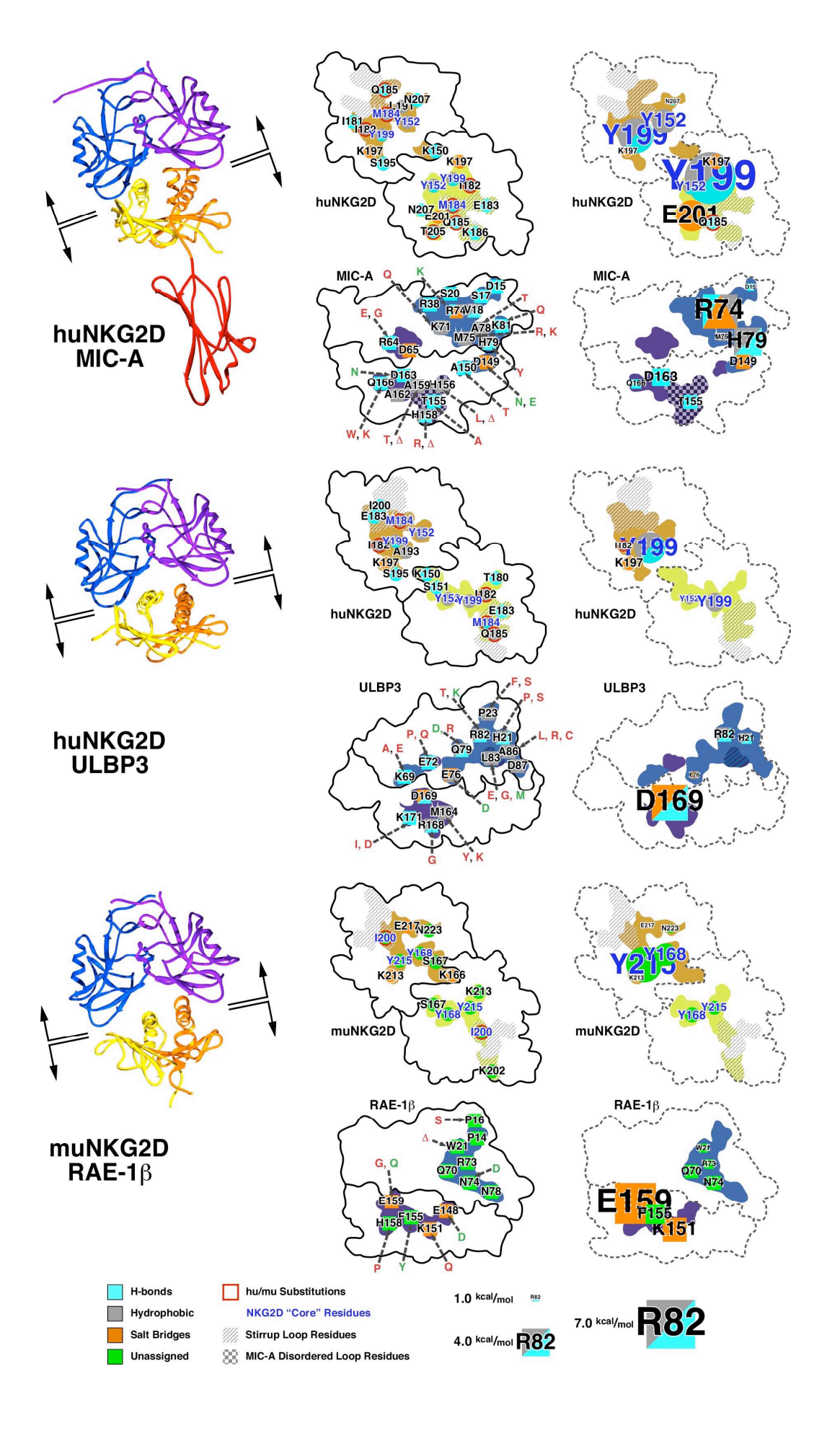


### **Figure 14.7** (previous page)

Schematization of NKG2D-ligand interfaces. Residues making contacts in the NKG2D-ligand complexes are represented schematically on outlines of the separated proteins involved in the interaction: huNKG2D-MIC-A (top),<sup>21</sup> huNKG2D-ULBP3 (middle)<sup>22</sup> and muNKG2D-RAE-1β (bottom).<sup>23</sup> On the left, the plane of the separation is indicated on ribbon representations of the complex structures, colored by domain as in Fig. 14.1. The interfaces are schematized by mapping the position of the contact residues (indicated by gnomons colored to reflect the nature of the bonds as indicated) onto outlines of the receptor (top) and the ligand (bottom). The overall footprint of one binding partner on the other is shown, colored by the domain making the footprint. Allelic and isoform substitutions affecting contact residues are indicated (conservative substitutions in green, non-conservative substitutions in red), as are portions of the receptors from stirrup loop residues (cross-hatched areas) and the portion of MIC-A from disordered loop residues (checkerboard area). The right-hand pair of interface schematics (dotted outlines)s shows the same contact residue mapping, but with residue gnomons now scaled (as indicated) by calculated  $\Delta\Delta G$  value;<sup>47</sup> residues with  $\Delta\Delta G$  values below the cut-off for the definition of binding 'hotspots' (1 kcal/mole) are not shown. Gnomons with red outlines highlight NKG2D ligand contacting residues where sequence differences occur between murine and huNKG2D; NKG2D sequence positions that are ligand contacts in all six half-sites (NKG2D 'core' residues) are indicated with blue labeling.

Thus, NKG2D has evolved to utilize a recognition mechanism that is capable of specifically binding to diverse ligands while tolerating considerable variation in ligand interfaces. The latter phenomenon may allow the immune system to fine-tune the NKG2D activation threshold through subtle alteration of the kinetics and affinities of particular interactions in specific contexts, allowing modulation of NKG2D signals through peripheral ligand sequence variation. This extreme degenerate recognition is achieved within an essentially rigid receptor binding site structure by a 'rigid adaptation' mechanism which complements the function of NKG2D:81 NKG2D is a dominantly activating immunoreceptor, where NKG2D engagement delivers strongly activating signals to effector cells that can override many, if not all, inhibitory signals. Utilizing rigid adaptation recognition in this context has the distinct advantage that the cross-reactivity inherent in induced-fit binding mechanisms<sup>8, 9, 85</sup> is prevented, while, at the same time, enabling recognition degeneracy to expand the repertoire of potential NKG2D ligands, extending NKG2D functionality to a variety of contexts. Inappropriate ligand engagement by NKG2D, through cross-reactivity, would result in the elimination of inappropriate target cells, with potentially serious physiological consequences. Thus, the immune system has developed an elegant system delivering broad utility while minimizing potentially deleterious responses, mirroring the functionally distinct recognition mechanisms utilized by TCRs or antibodies.

Human NKG2D	MIC-A Contact	Human NKG2D	ULBP3 Contact	Murine NKG2D	RAE-1β Contact
A-chain		A-chain		A-chain	
K150	x	K150	E76°‡	K166	x
S151	x	S151	Q79*	S167	Q70
\/450	к71°, <b>R74</b> *,		Q79°, <b>R82</b> *,	\/o	W21, Q70,
Y152	M75°	Y152	L83°	Y168	R73
T180	X X	T180	K69*	T196	x
I181	x	I181	X	L197	x
l182	H79°	l182	A86°, D87°	V198	x
E183	K81*	E183	H21*	E199	x
L100		L 103		L199	^
M184	v18*°, <b>R74</b> °,	M184	H21*°, R82°,	1200	P14
	A78°		A86°		
Q185	V18*	Q185	P23°	P201	х
K186	D15*, S17*	K186	х	K202	P16
L191	X	L191	X	V207	X
A193 S195	X X	A193 S195	X X	G209 S211	x x
K197	D149‡	K197	x	K213	N78
	-				
Y199	м75°, <b>H79</b> *	Y199	L83°	Y215	R73, N74
I200	_ X	I200	x	T216	X
E201	R74‡	E201	x	E217	X
T205	S20*	T205	х	N221	x
N207	R38*	N207	х	N223	Х
B-chain		B-chain		B-chain	
K150	A150*	K150	x	K166	E148‡
S151	Х	S151	Х	S167	E148
Y152	H156°, A159°	Y152	M164°	Y168	<b>K151</b> , F155
T180	X	T180	X	T196	X
l181	Q166*	l181	X	L197	X
l182	A162°, <b>Q166</b> °	l182	R168°	V198	X
E183		E183	K171*	E199	x
M184	H158°, A162°	M184	R168°, K171*	I200	H158
Q185	H158*	Q185	x	P201	x
K186	x	K186	x	K202	x
L191	T155°	L191	х	V207	x
A193	x	A193	L83°	G209	x
S195	R64*	S195	E72*	S211	x
K197	D65‡	K197	D169 <sub>‡</sub>	K213	E159 <sub>‡</sub>
			M164°, R168°,		F155,
Y199	A159°, <b>D163*</b>	Y199	D169*	Y215	E159
		1000			
1200	Х	1200	R168*	T216	X
E201	Х	E201	Х	E217	K151 <sub>‡</sub>
T205	X 	T205	X	N221	X
N207	T155*	N207	X	N223	K151

Hydrophobic/van der Waals interaction: °; hydrogen bond: \*; salt bridge: ‡

## **Figure 14.8** (previous page)

Tabulations of NKG2D-ligand contacts. Residues involved in receptor-ligand contacts are shown, separated by NKG2D monomer. Absence of a contact in one complex that is present in another is indicated ('x'). The nature of the bonding interaction is shown with symbols ( $^{\circ}$ ,  $^{*}$ ,  $^{\ddagger}$ ) as indicated (note that the resolution of the muNKG2D-RAE-1 $\beta$  complex was limited enough to restrict bond assignments). The calculated  $\Delta\Delta G$  value for easth residue is reflected in the font size as indicated:

≤ 1 kcal/mol ≤ 3 kcal/mol ≤ 5 kcal/mol > 5 kcal/mole

#### NKG2D: open questions

While the degree of sequence variation tolerated by NKG2D at ligand interfaces is remarkable, the picture for the ULBP ligands becomes more complicated. The sequence conservation among MIC proteins ( $\geq$ 84%) and RAE-1s ( $\geq$ 89%) is sufficiently high that the structures among family members are likely conserved to the degree that these ligands interact with NKG2D in very similar ways. Therefore, the assumption underlying Fig. 14.11, that receptor contact maps are valid across family members, is likely correct. However, the sequence conservation among the ULBPs ( $\geq$ 30%) is low enough that the underlying structures are almost certainly significantly different, invalidating the assumptions that the NKG2D interactions, and, therefore, contact maps, would be conserved across ULBP family members. This prediction is borne out by the analysis shown in Fig. 14.11, where the correlation between  $\Delta\Delta$ G value and degree of conservation (demonstrated by the MIC ligands) breaks down for the ULBPs. The conclusion is that the ULBP family may show considerable variation in structure and, therefore, interactions with NKG2D.

The NKG2D structures also present another conundrum: how is ligand engagement signaled through the ectodomain? The most flexible part of the receptor is the N-terminal stalk of the ectodomain between the CTLD and the membrane-spanning domain (NKG2x receptors are type II transmembrane proteins). These arms are among the more variable elements in the NKG2x NKR family (Fig. 14.12). Although the various crystallization constructs used in the crystallographic analyses encompass most, if not all, of this region, at most only about a quarter, and typically only a few residues, of the stalk is ordered in any of the five different crystal structures of NKG2D (human or mouse, free or complexed). However, while extremely flexible, the stalks do not contribute to 'induced-fit' recognition because they are distal to the ligand binding sites. Electron density is observed for more of the flexible N-terminal stalk in the free human NKG2D structure<sup>47</sup> than in any other structure. In this most fully resolved view, the stalk displays no defined secondary structure, and the only contacts between stalks of the same homodimer are van der Waals bonds near the interface between monomers in the homodimer. The extreme flexibility of the N-terminal stalk, and the lack of any obvious, consistent associations between stalks or stalk and CTLD, leaves us without an obvious structural mechanism for signaling ligand engagement to the cell's interior. The crystallographic analyses suggest that the receptor does not multimerize in any way relevant to signaling. No proteins have been identified that associate with any

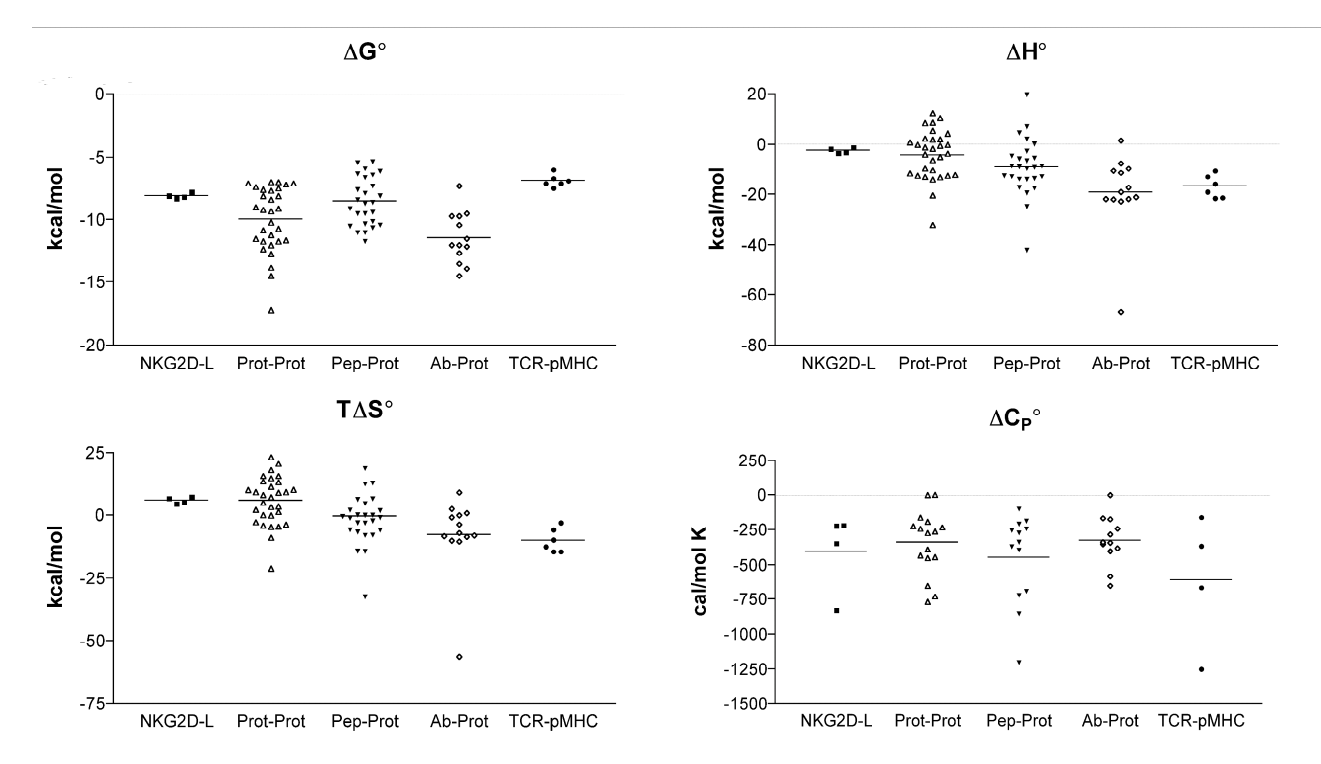
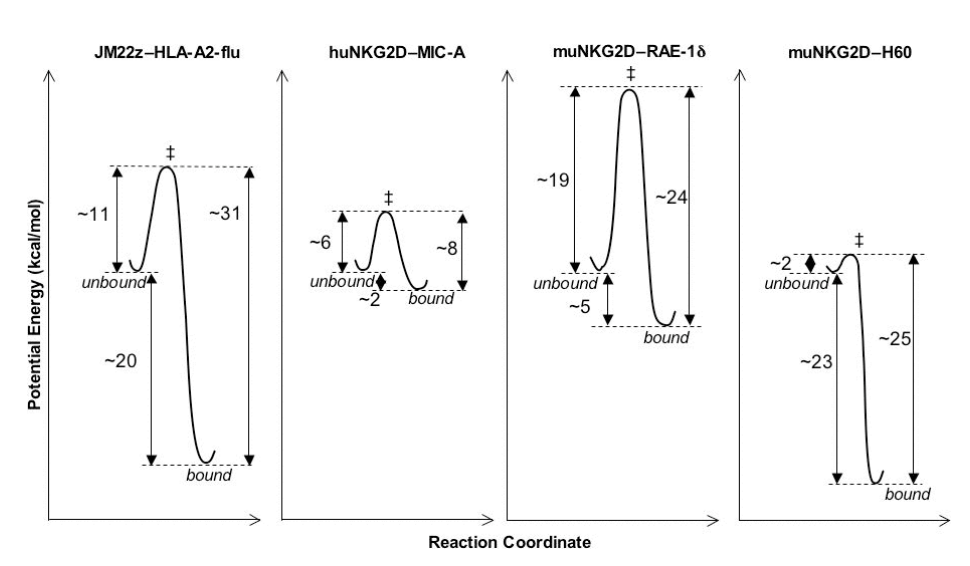


Figure 14.9

Thermodynamics of receptor–ligand interactions. Experimentally-derived values for  $\Delta G^{\circ}$ ,  $\Delta H^{\circ}$ ,  $T\Delta S^{\circ}$ , and  $\Delta C^{\circ}_{P}$  are shown for, from left to right: NKG2D–ligand interactions, rigid protein–rigid protein interactions (excluding antibodies), peptide–protein interactions, antibody–protein interactions (where the antibody is known to utilize induced-fit recognition) and  $\alpha\beta$  TCR–pMHC interactions. R1, R5-R9 Horizontal lines represent average values for each class. Values were measured in the range of 287.3 to 303K.



**Figure 14.10** 

Immunoreceptor–ligand binding energetics. Reaction energy profiles, to scale, of four representative immunoreceptor– ligand interactions: JM22z αβ TCR–HLA-A2–flu pMHC,<sup>87</sup> huNKG2D–MIC-A,<sup>81</sup> muNKG2D–RAE-1β and –H60.<sup>90</sup> All kinetic values were originally derived from SPR-determined association

and dissociation rate constants over a range of temperatures.  $E_a^{ass}$ , energy of association, is the transition from unbound state to the high-energy intermediate;  $E_a^{diss}$ , energy of dissociation, is the transition from the high-energy intermediate to the bound state; ‡, high-energy intermediate.

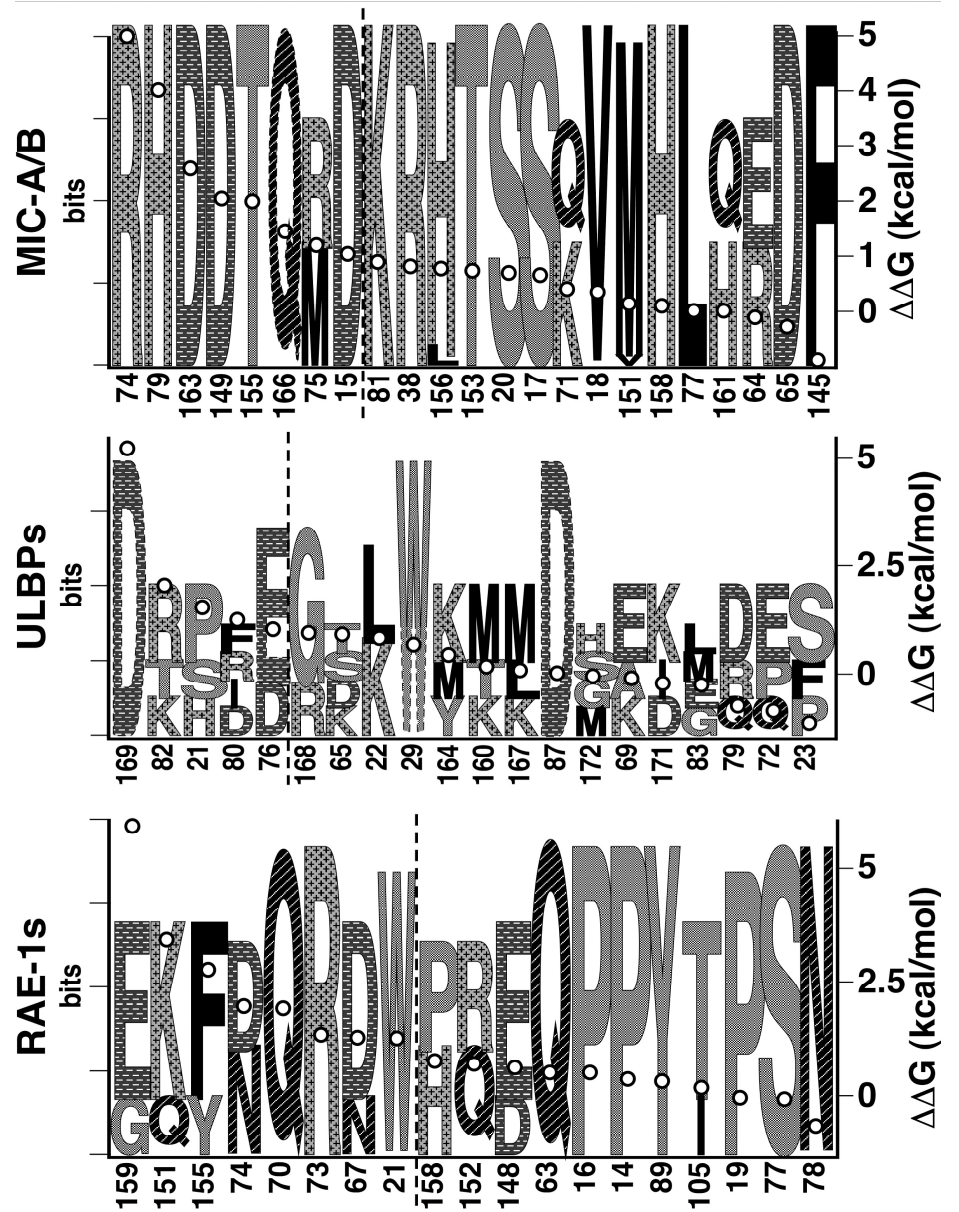


### **Figure 14.11**

Sequence variation NKG2D-ligand contact residues. The positions, in the sequence, of MIC (top), ULBP (middle) or RAE-1 (bottom) residues contacting NKG2D are plotted from left to right, in descending order of their associated contribution to NKG2D binding  $(\Delta \Delta G)$ , which is plotted as open circles (righthand ordinate). Sequence variation at NKG2D contacts due to allelic (MIC-A/B) and isoform (ULBP and RAE-1) substitutions is shown as sequence 'logos'. 91 Amino acids are shown in singleletter coding, patterned by The vertical dashed type. line indicates the 1 kcal/mole  $\Delta\Delta G$  cut-off, the accepted definition of the threshold for a binding 'hotspot'. The predicted pattern is readily

apparent for the MIC proteins, where increasing sequence variation correlates with decreasing  $\Delta\Delta G$  value. This pattern is superficially reversed for the RAE-1s, though not with closer inspection: the sequence substitutions associated with higher  $\Delta\Delta G$  values are either quite conservative or do not affect the contacts to backbone atoms. There is little pattern to the ULBPs, reflecting the proposition that the low sequence conservation (59 to 30%) among family members results in structural changes significant enough to invalidate the transfer of NKG2D contact maps from one family member to the next.

part, such as the unstructured arm, of the NKG2D ectodomain on the surface of effector cells that may contribute to a signal transduction mechanism.

## NKG2D: implications for NKG2x-CD94 recognition

A complex structure between NKG2x-CD94 receptors and HLA-E ligands has been modeled, in some detail, based on the NKG2D-MIC-A complex structure, 21, 39 extending a lower-resolution model based on the crystal structure of CD94.46 In this model, CD94 overlies the α1 domain of HLA-E, with a small hydrophobic patch on CD94 matching a similar patch on HLA-E (residues in the α1 domain and bound peptide at P8). There is no comparable hydrophobic patch on the α2 domain of HLA-E underlying the presumed position of the NKG2 moiety, but compensatory changes occur in the sequences of both NKG2A and NKG2C, thus accommodating this difference. The flatter NKG2x-CD94 binding surface complements the wider surface of HLA-E relative to the NKG2D ligands, where the platform interhelical distance is broadened by the bound, MHC class Ia-derived peptide. The side-chain of a conserved arginine at the P5 position in the peptide would also be able to exchange hydrogen bonds with residues from either NKG2x or CD94 at the homodimer interface. Fewer peptide side-chains are accessible in HLA-E complexes (mostly the P4, P5 and P8 residues, with P1 and P6 to a lesser extent) than MHC class Ia proteins due to the deeper, more encompassing, peptide groove. Residues in a loop of CD94 at the heterodimer interface are in position to reach into the peptide binding groove, hydrogen bonding to the peptide backbone at either P4 or P5. The comparable loop in NKG2D and Ly49A does not extend as far downward, toward the binding saddle, as in CD94. The restructuring of the  $\alpha$ 2 helix in CD94 into an extended loop (at the base of the homodimer interface in Fig. 14.2) accommodates the presence of a peptide in complex with the MHC protein. Four acidic residues in CD94 dominate a patch at the predicted interface matching a cluster of positively-charged residues on HLA-E and P5-arginine in the peptide. Using the CD94 homodimer and the structure of NKG2D to model an NKG2A-CD94 heterodimer results in a binding site on NKG2A that is dominated by charged and polar residues which would overlie a similarly charged surface on HLA-E, suggesting that the NKG2A-HLA-E interaction may be more similar in character to the KIR2DL2-pMHC and Ly49A-pMHC interactions, which are dominated by complementary charge-charge interactions, than to NKG2D-MIC-A binding. This is consistent with the different recognition mechanisms employed by NKG2D and the other receptors of the NKG2x family: where NKG2D displays extreme recognition degeneracy, the NKG2x-CD94 receptors are expected to display much more typical, highly-specific, protein-protein recognition since their ligand repertoire is so much more limited. However, these models are not good enough to completely delineate the role peptide plays in recognition. It is also clear that the peptide can have indirect effects on receptor interactions; substitutions at the P2 position can markedly affect the thermal stability of HLA-E, mostly through the introduction of cavities, that subsequently affects both cellsurface expression levels and receptor interactions.<sup>39</sup>



### **Figure 14.12**

Comparison of NKG2x N-terminal ectodomain arm sequences. Alignments were calculated with CLUSTALW.<sup>49</sup>

### MIC & γδ TCRs

Aside from its role as a ligand for NKG2D, MIC proteins are also directly recognized by γδ TCRs of the Vδ1 subset. 92 Unlike αβ TCRs, which only interact with peptide fragments of protein antigens presented as complexes with MHC class I molecules, γδ TCRs are proposed to interact directly with intact antigens, apparently without the requirement of extensive processing 93-97 – though considerably less is known about the functional details of this class of TCR. In humans, γδ T cells can be functionally divided on the basis of the Vδ gene utilization of the expressed γδ TCR. Vδ2Vγ9 T cells predominate in the peripheral blood and are thought to provide anti-bacterial defenses by directly recognizing soluble, mycobacterially-derived prenyl pyrophosphate and alkamine compounds. 97-101 Both on the basis of the distribution of CDR sequence variation and the crystal structure of a Vδ2Vγ9 TCR, γδ TCRs are proposed to interact with and recognize ligands more like antibodies than αβ TCRs. 97, 102, 103 The scarcer Vδ1-bearing T cells are enriched in the epithelial compartment, 104, 105 paralleling the restricted tissue distribution of MIC proteins. Previously, it had been shown that Vδ1 γδ T cell lines recognize and kill MIC-bearing targets, and that this interaction could be blocked by anti-γδ TCR antibodies.<sup>54, 56, 58, 64</sup> But, since these cells also express MIC-specific NKG2D receptors, it was not clear that a direct interaction between MIC and V $\delta$ 1 y $\delta$  TCR occurred and drove activation prior to the aforementioned report. <sup>92</sup> The possibility also exists that Vδ1 γδ TCR-NKG2D-MIC form receptor-co-receptor-ligand complexes analogous to αβ TCR-CD8-pMHC complexes, possibly accommodated by the length and flexibility of the NKG2D N-terminal arm. This could require that the yoTCR interact with MIC at a site not overlapping with the NKG2D-interaction site.

In conclusion, though our understanding of the roles that NKG2D plays in mediating responses of the innate and adaptive immune systems is continuing to expand, it is already clear that this immunoreceptor uses unique, almost unprecedented recognition machinery to accomplish these tasks. Therefore, the principles of NKG2D immunorecognition represent a wholly distinct paradigm from that of TCR–ligand recognition, which together define two poles of protein–protein interactions employed to accomplish the disparate functions of the immune system.

#### References

- 1. Germain RN, Margulies DH. The biochemistry and cell biology of antigen processing and presentation. Annual Review of Immunology 1993;11:403-50.
- 2. Bjorkman PJ, Parham P. Structure, function and diversity of class I major histocompatibility complex molecules. Ann. Rev. Biochem. 1990;90:253-88.
- 3. Garcia KC, Degano M, Speir JA, Wilson IA. Emerging principles for T cell receptor recognition of antigen in cellular immunity. Reviews in Immunogenetics 1999;1:75 90.
- 4. Lenschow DJ, Walunas TL, Bluestone JA. CD28/B7 system of T cell costimulation. Annual Review of Immunology 1996;14:233-58.
- 5. Grakoui A, Bromley SK, Sumen C, Davis MM, Shaw AS, Allen PM, et al. The immunological synapse: a molecular machine controlling T cell activation. Science 1999;285(5425):221-7.
- 6. Koshland DE, Jr. Mechanism of Transfer Enzymes. In: *al.* PBe, editor. The Enzymes. Revised ed. New York: Academic Press; 1958. p. 305-315.
- 7. Sundberg EJ, Mariuzza RA. Luxury accommodations: the expanding role of structural plasticity in protein-protein interactions. Structure Fold Des 2000;8(7):R137-42.
- 8. James LC, Roversi P, Tawfik DS. Antibody multispecificity mediated by conformational diversity. Science 2003;299(5611):1362-7.
- 9. Wu LC, Tuot DS, Lyons DS, Garcia KC, Davis MM. Two-step binding mechanism for T-cell receptor recognition of peptide MHC. Nature 2002;418(6897):552-6.
- 10. Trinchieri G. Biology of natural killer cells. Adv. Immunol. 1989;47:187 376.
- 11. Yokoyama WM, Plougastel BF. Immune functions encoded by the natural killer gene complex. Nat Rev Immunol 2003;3(4):304-16.
- 12. Held W, Coudert JD, Zimmer J. The NK cell receptor repertoire: formation, adaptation and exploitation. Curr Opin Immunol 2003;15(2):233-7.
- 13. Diefenbach A, Raulet DH. Innate immune recognition by stimulatory immunoreceptors. Curr Opin Immunol 2003;15(1):37-44.
- 14. Bakker AB, Wu J, Phillips JH, Lanier LL. NK cell activation: distinct stimulatory pathways counterbalancing inhibitory signals. Human Immunology 2000;61(1):18-27.
- 15. Diefenbach A, Raulet DH. Strategies for target cell recognition by natural killer cells. Immunol Rev 2001;181:170-84.
- 16. Raulet DH, Vance RE, McMahon CW. Regulation of the natural killer cell receptor repertoire. Annual Review of Immunology 2001;19:291-330.
- 17. Lanier LL. Turning on natural killer cells. Journal of Experimental Medicine 2000;191(8):1259-62.
- 18. Garboczi DN, Ghosh P, Utz U, Fan QR, Biddison WE, Wiley DC. Structure of the complex between human T-cell receptor, viral peptide and HLA-A2. Nature 1996;384(6605):134-41.
- 19. Boyington JC, Motyka SA, Schuck P, Brooks AG, Sun PD. Crystal structure of an NK cell immunoglobulin-like receptor in complex with its class I MHC ligand. Nature 2000;405(6786):537-43.
- 20. Tormo J, Natarajan K, Margulies DH, Mariuzza RA. Crystal structure of a lectin-like natural killer cell receptor bound to its MHC class I ligand. Nature 1999;402:623 631.
- 21. Li P, Morris DL, Willcox BE, Steinle A, Spies T, Strong RK. Complex Structure of the Activating Immunoreceptor NKG2D and its MHC Class I-like Ligand MICA. Nature Immunol. 2001;2:443 451.

- 22. Radaev S, Rostro B, Brooks AG, Colonna M, Sun PD. Conformational plasticity revealed by the cocrystal structure of NKG2D and its class I MHC-like ligand ULBP3. Immunity 2001;15(6):1039-49.
- 23. Li P, McDermott G, Strong RK. Crystal structures of RAE-1beta and its complex with the activating immunoreceptor NKG2D. Immunity 2002;16(1):77-86.
- 24. Colonna M. Immunoglobulin superfamily inhibitory receptors: from natural killer cells to antigen-presenting cells. Res Immunol 1997;148(3):169-71.
- 25. Karlhofer FM, Ribaudo RK, Yokoyama WM. MHC class I alloantigen specificity of Ly-49+ IL-2-activated natural killer cells. Nature 1992;358(6381):66-70.
- 26. Weis WI, Taylor ME, Drickamer K. The C-type lectin superfamily in the immune system. Immunological Reviews 1998;163:19-34.
- 27. Drickamer K. C-type lectin-like domains. Current Opinion in Structural Biology 1999;9(5):585-90.
- 28. Drickamer K. Ca<sup>2+</sup>-dependent carbochydrate-recognition domains in animal proteins. Curr. Opin. Struct. Biol. 1993;3:393 400.
- 29. Uhrberg M, Parham P, Wernet P. Definition of gene content for nine common group B haplotypes of the Caucasoid population: KIR haplotypes contain between seven and eleven KIR genes. Immunogenetics 2002;54(4):221-9.
- 30. Makrigiannis AP, Pau AT, Schwartzberg PL, McVicar DW, Beck TW, Anderson SK. A BAC contig map of the Ly49 gene cluster in 129 mice reveals extensive differences in gene content relative to C57BL/6 mice. Genomics 2002;79(3):437-44.
- 31. Uhrberg M, Valiante NM, Shum BP, Shilling HG, Lienert-Weidenbach K, Corliss B, et al. Human diversity in killer cell inhibitory receptor genes. Immunity 1997;7(6):753-63.
- 32. Kubota A, Kubota S, Lohwasser S, Mager DL, Takei F. Diversity of NK cell receptor repertoire in adult and neonatal mice. Journal of Immunology 1999;163(1):212-6.
- 33. Ohlen C, Kling G, Hoglund P, Hansson M, Scangos G, Bieberich C, et al. Prevention of allogeneic bone marrow graft rejection by H-2 transgene in donor mice. Science 1989;246(4930):666-8.
- 34. Bauer S, Groh V, Wu J, Steinle A, Phillips JH, Lanier LL, et al. Activation of NK cells and T cells by NKG2D, a receptor for stress-inducible MICA. Science 1999;285(5428):727-9.
- 35. Wu J, Song Y, Bakker AB, Bauer S, Spies T, Lanier LL, et al. An activating immunoreceptor complex formed by NKG2D and DAP10. Science 1999;285(5428):730-2.
- 36. Borrego F, Kabat J, Kim D-K, Lieto L, Maasho K, Peña J, et al. Structure and function of major histocompatibility complex (MHC) class I specific receptors expressed on human natural killer (NK) cells. Molecular Immunology 2002;1063:1 24.
- 37. Plougastel B, Trowsdale J. Cloning of NKG2-F, a new member of the NKG2 family of human natural killer cell receptor genes. European Journal of Immunology 1997;27(11):2835-9.
- 38. O'Callaghan CA, Tormo J, Willcox BE, Braud VM, Jakobsen BK, Stuart DI, et al. Structural features impose tight peptide binding specificity in the nonclassical MHC molecule HLA-E. Molecular Cell 1998;1(4):531-41.
- 39. Strong RK, Holmes MA, Li P, Braun-Jones L, Lee N, Geraghty DE. HLA-E allelic variants: Correlating differential expression, peptide affinities, crystal structures and thermal stabilities. J Biol Chem 2002.
- 40. Lee N, Goodlett DR, Ishitani A, Marquardt H, Geraghty DE. HLA-E surface expression depends on binding of TAP-dependent peptides derived from certain HLA class I signal sequences. J Immunol 1998;160(10):4951-60.

- 41. Plougastel B, Jones T, Trowsdale J. Genomic structure, chromosome location, and alternative splicing of the human NKG2A gene. Immunogenetics 1996;44(4):286-91.
- 42. Bellon T, Heredia AB, Llano M, Minguela A, Rodriguez A, Lopez-Botet M, et al. Triggering of effector functions on a CD8+ T cell clone upon the aggregation of an activatory CD94/kp39 heterodimer. Journal of Immunology 1999;162(7):3996-4002.
- 43. Lanier LL, Corliss B, Wu J, Phillips JH. Association of DAP12 with activating CD94/NKG2C NK cell receptors. Immunity 1998;8(6):693-701.
- 44. Lanier LL, Corliss BC, Wu J, Leong C, Phillips JH. Immunoreceptor DAP12 bearing a tyrosine-based activation motif is involved in activating NK cells. Nature 1998;391(6668):703 707.
- 45. Llera AS, Viedma F, Sanchez-Madrid F, Tormo J. Crystal structure of the C-type lectin-like domain from the human hematopoietic cell receptor CD69. J Biol Chem 2001;276(10):7312-9.
- 46. Boyington JC, Riaz AN, Patamawenu A, Coligan JE, Brooks AG, Sun PD. Structure of CD94 reveals a novel C-type lectin fold: implications for the NK cell-associated CD94/NKG2 receptors. Immunity 1999;10(1):75-82.
- 47. McFarland BJ, Kortemme T, Yu SF, Baker D, Strong RK. Symmetry Recognizing Asymmetry. Analysis of the Interactions between the C-Type Lectin-like Immunoreceptor NKG2D and MHC Class I-like Ligands. Structure (Camb) 2003;11(4):411-22.
- 48. Feinberg H, Park-Snyder S, Kolatkar AR, Heise CT, Taylor ME, Weis WI. Structure of a C-type carbohydrate recognition domain from the macrophage mannose receptor. J Biol Chem 2000;275(28):21539-48.
- 49. Thompson JD, Higgins DG, Gibson TJ. CLUSTAL W: improving the sensitivity of progressive multiple sequence alignment through sequence weighting, position-specific gap penalties and weight matrix choice. Nucleic Acids Res 1994;22(22):4673-80.
- 50. Steinle A, Li P, Morris DL, Groh V, Lanier LL, Strong RK, et al. Interactions of human NKG2D with its ligands MICA, MICB, and homologs of the mouse RAE-1 protein family. Immunogenetics 2001;53:279 287.
- 51. Wu J, Cherwinski H, Spies T, Phillips JH, Lanier LL. DAP10 and DAP12 form distinct, but functionally cooperative, receptor complexes in Natural Killer cells. J. Exp. Med. 2000;192:1059 1067.
- 52. Gilfillan S, Ho EL, Cella M, Yokoyama WM, Colonna M. NKG2D recruits two distinct adapters to trigger NK cell activation and costimulation. Nat Immunol 2002;3(12):1150-5.
- 53. Diefenbach A, Tomasello E, Lucas M, Jamieson AM, Hsia JK, Vivier E, et al. Selective associations with signaling proteins determine stimulatory versus costimulatory activity of NKG2D. Nat Immunol 2002;3(12):1142-9.
- 54. Bahram S, Bresnahan M, Geraghty DE, Spies TA. A second lineage of mammalian major histocompatibility complex class I genes. Proc. Natl. Acad. Sci. USA 1994;91:6259 6263.
- 55. Bahram S, Spies TA. Nucleotide sequence of a human *MHC* class I *MICB* cDNA. Immunogenetics 1996;43:230 233.
- 56. Groh V, Bahram S, Bauer S, Herman A, Beauchamp M, Spies T. Cell stress-regulated human major histocompatibility complex class I gene expressed in gastrointestinal epithelium. Proc. Natl. Acad. Sci. USA 1996;93:12445 12450.
- 57. Cosman D, Mullberg J, Sutherland CL, Chin W, Armitage R, Fanslow W, et al. ULBPs, novel MHC class I-related molecules, bind to CMV glycoprotein UL16 and stimulate NK cytotoxicity through the NKG2D receptor. Immunity 2001;14(2):123-33.
- 58. Groh V, Steinle A, Bauer S, Spies T. Recognition of Stess-Induced MHC Molecules by Intestinal Epithelial γδ T Cells. Science 1998;279:1737 1740.

- 59. Diefenbach A, Jamieson AM, Liu SD, Shastri N, Raulet DH. Ligands for the murine NKG2D receptor: expression by tumor cells and activation of NK cells and macrophages. Nature Immunology 2000;1(2):119-26.
- 60. Jamieson AM, Diefenbach A, McMahon CW, Xiong N, Carlyle JR, Raulet DH. The role of the NKG2D immunoreceptor in immune cell activation and natural killing. Immunity 2002;17(1):19-29.
- 61. Cerwenka A, Bakker AB, McClanahan T, Wagner J, Wu J, Phillips JH, et al. Retinoic acid early inducible genes define a ligand family for the activating NKG2D receptor in mice. Immunity 2000;12(6):721-7.
- 62. Diefenbach A, Jensen ER, Jamieson AM, Raulet DH. Rae1 and H60 ligands of the NKG2D receptor stimulate tumour immunity. Nature 2001;413:165 171.
- 63. Pende D, Cantoni C, Rivera P, Vitale M, Castriconi R, Marcenaro S, et al. Role of NKG2D in tumor cell lysis mediated by human NK cells: cooperation with natural cytotoxicity receptors and capability of recognizing tumors of nonepithelial origin. Eur J Immunol 2001;31(4):1076-86.
- 64. Groh V, Rhinehart R, Secrist H, Bauer S, Grabstein KH, Spies T. Broad tumor-associated expression and recognition by tumor-derived gamma delta T cells of MICA and MICB. Proc. Natl. Acad. Sci. USA 1999;96(12):6879-84.
- 65. Bahram S, Mizuki N, Inoko H, Spies TA. Nucleotide sequence of the human MHC class I *MICA* gene. Immunogenetics 1996;44:80 81.
- 66. Stephens HA. MICA and MICB genes: can the enigma of their polymorphism be resolved? Trends in Immunology 2001;22(7):378 385.
- 67. Holmes MA, Li P, Petersdorf EW, Strong RK. Structural studies of allelic diversity of the MHC class I homolog MIC-B, a stress-inducible ligand for the activating immunoreceptor NKG2D. J Immunol 2002;169(3):1395-400.
- 68. Groh V, Wu J, Yee C, Spies T. Tumour-derived soluble MIC ligands impair expression of NKG2D and T-cell activation. Nature 2002;419(6908):734-8.
- 69. Salih HR, Rammensee HG, Steinle A. Cutting edge: down-regulation of MICA on human tumors by proteolytic shedding. J Immunol 2002;169(8):4098-102.
- 70. Welte SA, Sinzger C, Lutz SZ, Singh-Jasuja H, Sampaio KL, Eknigk U, et al. Selective intracellular retention of virally induced NKG2D ligands by the human cytomegalovirus UL16 glycoprotein. Eur J Immunol 2003;33(1):194-203.
- 71. Zou Z, Nomura M, Takihara Y, Yasunaga T, Shimada K. Isolation and characterization of retinoic acid-inducible cDNA clones in F9 cells: a novel cDNA family encodes cell surface proteins sharing partial homology with MHC class I molecules. Journal of Biochemistry 1996;119(2):319-28.
- 72. Carayannopoulos LN, Naidenko OV, Fremont DH, Yokoyama WM. Cutting edge: murine UL16-binding protein-like transcript 1: a newly described transcript encoding a high-affinity ligand for murine NKG2D. J Immunol 2002;169(8):4079-83.
- 73. Nomura M, Zou Z, Joh T, Takihara Y, Matsuda Y, Shimada K. Genomic structures and characterization of Rae1 family members encoding GPI-anchored cell surface proteins and expressed predominantly in embryonic mouse brain. Journal of Biochemistry 1996;120(5):987-95.
- 74. Girardi M, Oppenheim DE, Steele CR, Lewis JM, Glusac E, Filler R, et al. Regulation of cutaneous malignancy by gammadelta T cells. Science 2001;294(5542):605-9.
- 75. Carayannopoulos LN, Naidenko OV, Kinder J, Ho EL, Fremont DH, Yokoyama WM. Ligands for murine NKG2D display heterogeneous binding behavior. Eur J Immunol 2002;32(3):597-605.

- 76. Malarkannan S, Shih PP, Eden PA, Horng T, Zuberi AR, Christianson G, et al. The molecular and functional characterization of a dominant minor H antigen, H60. Journal of Immunology 1998;161(7):3501-9.
- 77. Malarkannan S, Horng T, Eden P, Gonzalez F, Shih P, Brouwenstijn N, et al. Differences that matter: major cytotoxic T cell-stimulating minor histocompatibility antigens. Immunity 2000;13(3):333-44.
- 78. Farag SS, Fehniger TA, Ruggeri L, Velardi A, Caligiuri MA. Natural killer cell receptors: new biology and insights into the graft-versus-leukemia effect. Blood 2002;100(6):1935-47.
- 79. Lawrence M, Colman PM. Shape complementarity at protein/protein interfaces. J. Mol. Biol. 1993;234:946 950.
- 80. Willcox BE, Thomas LM, Bjorkman PJ. Crystal structure of HLA-A2 bound to LIR-1, a host and viral major histocompatibility complex receptor. Nat Immunol 2003;4(9):913-9.
- 81. McFarland BJ, Strong RK. Thermodynamic Analysis of Degenerate Recognition by the NKG2D Immunoreceptor: Not 'Induced Fit' but 'Rigid Adaptation'. Immunity *in press*.
- 82. Clackson T, Wells JA. A hot spot of binding energy in a hormone-receptor interface. Science 1995;267(5196):383-6.
- 83. Padlan EA. On the nature of antibody combining sites: unusual structural features that may confer on these sites an enhanced capacity for binding ligands. Proteins 1990;7(2):112-24.
- 84. Nikula TK, Bocchia M, Curcio MJ, Sgouros G, Ma Y, Finn RD, et al. Impact of the high tyrosine fraction in complementarity determining regions: measured and predicted effects of radioiodination on IgG immunoreactivity. Mol Immunol 1995;32(12):865-72.
- 85. Boniface JJ, Reich Z, Lyons DS, Davis MM. Thermodynamics of T cell receptor binding to peptide-MHC: evidence for a general mechanism of molecular scanning. Proc Natl Acad Sci U S A 1999;96(20):11446-51.
- 86. Stites WE. Protein-protein interactions: Interface structure, binding thermodynamics, and mutational analysis. Chem. Rev. 1997;97(5):1233-1250.
- 87. Willcox BE, Gao GF, Wyer JR, Ladbury JE, Bell JI, Jakobsen BK, et al. TCR binding to peptide-MHC stabilizes a flexible recognition interface. Immunity 1999;10(3):357-65.
- 88. Garcia KC, Radu CG, Ho J, Ober RJ, Ward ES. Kinetics and thermodynamics of T cell receptor- autoantigen interactions in murine experimental autoimmune encephalomyelitis. Proc Natl Acad Sci U S A 2001;98(12):6818-23.
- 89. Anikeeva N, Lebedeva T, Krogsgaard M, Tetin SY, Martinez-Hackert E, Kalams SA, et al. Distinct Molecular Mechanisms Account for the Specificity of Two Different T-Cell Receptors. Biochemistry 2003;42(16):4709-4716.
- 90. O'Callaghan CA, Cerwenka A, Willcox BE, Lanier LL, Bjorkman PJ. Molecular competition for NKG2D: H60 and RAE1 compete unequally for NKG2D with dominance of H60. Immunity 2001;15:201-211.
- 91. Schneider TD, Stephens RM. Sequence logos: a new way to display consensus sequences. Nucleic Acids Res 1990;18(20):6097-100.
- 92. Wu J, Groh V, Spies T. T Cell Antigen Receptor Engagement and Specificity in the Recognition of Stress-Inducible MHC Class I-Related Chains by Human Epithelial  $\gamma\delta$  T Cells. Journal of Immunology 2002;169:1236-1240.
- 93. Porcelli S, Brenner MB, Band H. Biology of the human gamma delta T-cell receptor. Immunological Reviews 1991;120:137-83.
- 94. Schild H, Mavaddat N, Litzenberger C, Ehrich EW, Davis MM, Bluestone JA, et al. The nature of major histocompatibility complex recognition by gamma delta T cells. Cell 1994;76(1):29-37.

- 95. Morita CT, Beckman EM, Bukowski JF, Tanaka Y, Band H, Bloom BR, et al. Direct presentation of nonpeptide prenyl pyrophosphate antigens to human gamma delta T cells. Immunity 1995;3(4):495-507.
- 96. Davis MM, Boniface JJ, Reich Z, Lyons D, Hampl J, Arden B, et al. Ligand recognition by alpha beta T cell receptors. Annual Review of Immunology 1998;16:523-44.
- 97. Allison TJ, Garboczi DN. Structure of gd T cell receptors and their recognition of non-peptide antigens. Molecular Immunology 2002;38:1051-1061.
- 98. Constant P, Davodeau F, Peyrat MA, Poquet Y, Puzo G, Bonneville M, et al. Stimulation of human gamma delta T cells by nonpeptidic mycobacterial ligands. Science 1994;264(5156):267-70.
- 99. Bukowski JF, Morita CT, Tanaka Y, Bloom BR, Brenner MB, Band H. V gamma 2V delta 2 TCR-dependent recognition of non-peptide antigens and Daudi cells analyzed by TCR gene transfer. Journal of Immunology 1995;154(3):998-1006.
- 100. Tanaka Y, Morita CT, Nieves E, Brenner MB, Bloom BR. Natural and synthetic non-peptide antigens recognized by human gamma delta T cells. Nature 1995;375(6527):155-8.
- 101. Bukowski JF, Morita CT, Brenner MB. Human gamma delta T cells recognize alkylamines derived from microbes, edible plants, and tea: implications for innate immunity. Immunity 1999;11(1):57-65.
- 102. Rock EP, Sibbald PR, Davis MM, Chien YH. CDR3 length in antigen-specific immune receptors. Journal of Experimental Medicine 1994;179(1):323-8.
- 103. Allison TJ, Winter CC, Fournié J-J, Bonneville M, Garboczi DN. Structure of a human γδ T-cell antigen receptor. Nat. Immunol. 2001;411:820-24.
- 104. Spencer J, Isaacson PG, Diss TC, MacDonald TT. Expression of disulfide-linked and non-disulfide-linked forms of the T cell receptor gamma/delta heterodimer in human intestinal intraepithelial lymphocytes. European Journal of Immunology 1989;19(7):1335-8.
- 105. Deusch K, Luling F, Reich K, Classen M, Wagner H, Pfeffer K. A major fraction of human intraepithelial lymphocytes simultaneously expresses the gamma/delta T cell receptor, the CD8 accessory molecule and preferentially uses the V delta 1 gene segment. Eur J Immunol 1991;21(4):1053-9.